

Structural diradical character

B. Alexander Voigt,¹ Torben Steenbock,¹ and Carmen Herrmann^{1, a)}

*Institute for Inorganic and Applied Chemistry, Martin-Luther-King-Platz 6,
University of Hamburg, 20146 Hamburg, Germany*

(Dated: 22 July 2022)

A reliable first-principles description of singlet diradical character is essential for predicting nonlinear optical and magnetic properties of molecules. Since diradical and closed-shell electronic structures differ in their distribution of single, double, and triple bonds, modeling electronic diradical character requires accurate bond-length patterns. A generally applicable measure for comparing first-principles bond-length patterns with experimental ones is not available at present. For this purpose, we introduce a new measure for structural (rather than electronic) diradical character. It has the advantage of being easily applicable to both computed and experimental molecular structures for arbitrary systems. Within Kohn–Sham density functional theory, we employ this measure for evaluating the suitability of four popular approximate exchange–correlation functionals with different exact-exchange admixtures (BP86, TPSS, B3LYP, TPSSh) for describing experimentally characterized organometallic and organic structures at the diradical / closed-shell border. The two hybrid functionals TPSSh and B3LYP perform best for diradical bond length patterns, with TPSSh being best for the organometallic reference systems and B3LYP for the organic ones. Still, none of the functionals is suitable for correctly describing relative bond lengths across the range of molecules studied, so that none can be recommended for predictive studies of (potential) diradicals without reservation. This underlines the importance of structural diradical character as a test for the further evaluation and development of electronic structure methods.

^{a)}Electronic mail: Carmen.Herrmann@chemie.uni-hamburg.de

I. INTRODUCTION

Open-shell singlet diradical molecules have aroused interest among both theoreticians and experimentalists due to their special physical and chemical properties.¹⁻¹⁰ Among those are their nonlinear optical (NLO) properties, especially the second hyperpolarizability, which can be tuned and amplified by a change in open-shell diradical character y ^{11,12}. Nonlinear optically active molecular materials are important for applications such as data storage and telecommunication¹³.

It would be particularly useful if the NLO properties of molecules or molecular materials could be switched by external stimuli. There has been considerable experimental¹⁴⁻¹⁸ and theoretical^{15,19-22} work on switchable organic and organometallic NLO-active molecules, showing that a variety of stimuli such as pH, temperature, redox reactions, and light can be used for this purpose.

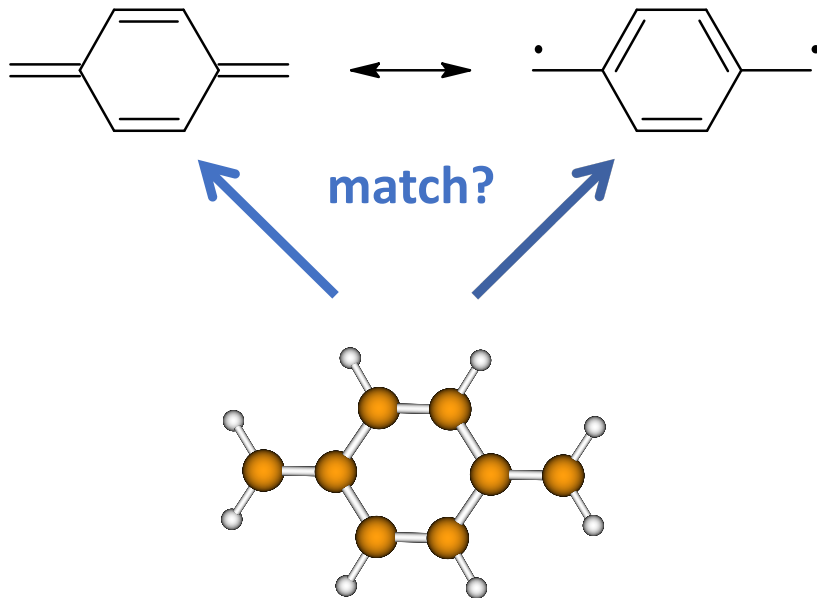


FIG. 1. Our measure of structural diradical character is based on comparing bond-length patterns of molecular structures with idealized bond-length patterns for closed- (top left) and open-shell diradical (top right) forms, shown here for p-quinodimethane. Note that strictly speaking, these are not mesomeric forms, since bond lengths will differ between the diradicaloid and the closed-shell structures.

First-principles modeling such as Kohn-Sham (KS)-density functional theory (DFT) is

essential for understanding structure–property relationships and for designing switchable functionality in such compounds²³, but if the electronic structures of the systems are not properly described, one may easily get incorrect optimized molecular structures and properties. Since the diradical character is related to the relative weights of open-shell and closed-shell singlet configurations in the electronic wave function^{24–27}, this issue is particularly crucial if structural parameters such as bond lengths differ between the closed-shell and the open-shell form (compare Figure 1). Indeed, it has been shown that diradical character and NLO properties can be very sensitive to molecular structure^{28–31}. Open-shell electronic structures have also been found to depend on interatomic distances in the context of strongly correlated adsorbates and materials^{32–34}.

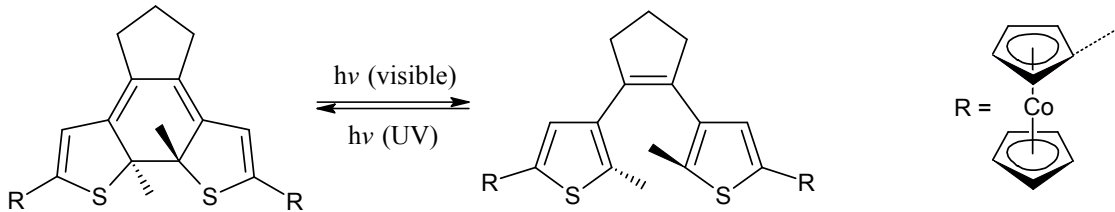


FIG. 2. Lewis structures of a dithienylethene molecule in its closed (left) and open form (right).

Given the favorable switching properties of dithienylethene (DTE) and the potential of metallocenes for redox-switchable NLO properties, a DTE bridge linking two cobaltocene units (with potentially one unpaired electron each) could be an interesting organometallic candidate for a multiresponse NLO-active compound (see Figure 2). Closing the photo-switch (left-hand side of Figure 2) switches on electronic communication via the π system of the bridge, which enables drawing two different structures, a closed-shell and an open-shell one (Figure 3). The relative importance of these two not only affects NLO properties, but a stabilization of the closed switch resulting from a large admixture of the closed-shell form can also suppress photochromic ring opening^{35,36}. Due to its poor switching behavior, the closed-switch form could not be isolated, and its structure and properties are not known experimentally³⁷. To decide whether further efforts towards obtaining these data and towards optimizing the switching behavior are worthwhile, we aim at a true first-principles prediction of the diradical character of the closed switch. In contrast to the analogous nitronyl nitroxide compound³⁸ (see Supplemental Material), KS-DFT optimizations of the molecular structure for the closed switch in its singlet state give no consistent answer to whether it is

predominantly a closed-shell or an open-shell structure. Consequently, no predictions of its diradical character and its NLO properties appear possible, unless a particular approximate exchange–correlation functional can be identified as sufficiently reliable for this purpose.

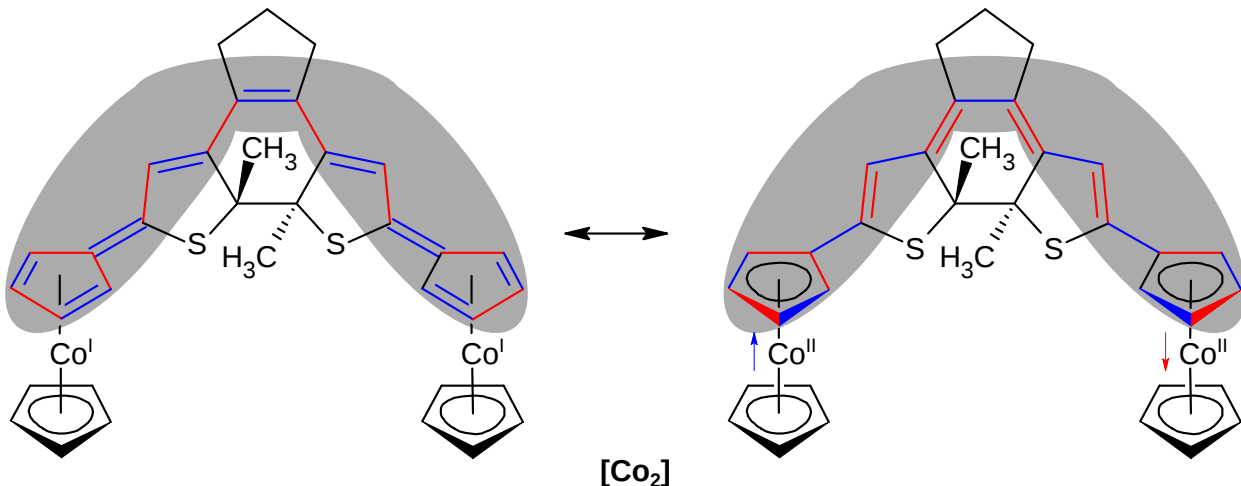


FIG. 3. Lewis structures of $[\text{Co}_2]$. The closed-shell quinoidal form is shown on the left-hand side, the diradicaloid form on the right-hand side. Note that strictly speaking, these are not mesomeric forms, since bond lengths will differ between the diradicaloid and the closed-shell structures. The bonds whose formal bond orders and thus lengths differ between the two structures are indicated by the grey area. Bonds included in evaluating established BLA measures are shown in red if they were added and in blue if they were subtracted in Eq. (1)^{39,40}.

For organic diradicals, the B3LYP exchange–correlation functional (with 20 % exact exchange admixture) generally works well⁴¹, but even here, BLA^{39,40} as present in the closed-shell form on the left-hand side of Figure 1 can be underestimated⁴² or overestimated^{30,43}, depending on the molecule studied. While numerous studies on the dependence of NLO properties on exchange–correlation functional have been carried out^{29,44–58}, it is not clear if there is a reasonably reliable functional for describing bond length patterns for organometallic complexes with potential diradical character. Also, there is no uniquely defined measure for bond length alternation for compounds in which there is not an even number of alternating carbon–carbon single and double (or triple) bonds, for example the organometallic complexes shown in Figure 3, for cyanobutadiynyl complexes⁵⁹, or for the tin clusters studied in Ref.⁶⁰.

Below, we define such a measure for bond length patterns applicable to arbitrary chemical

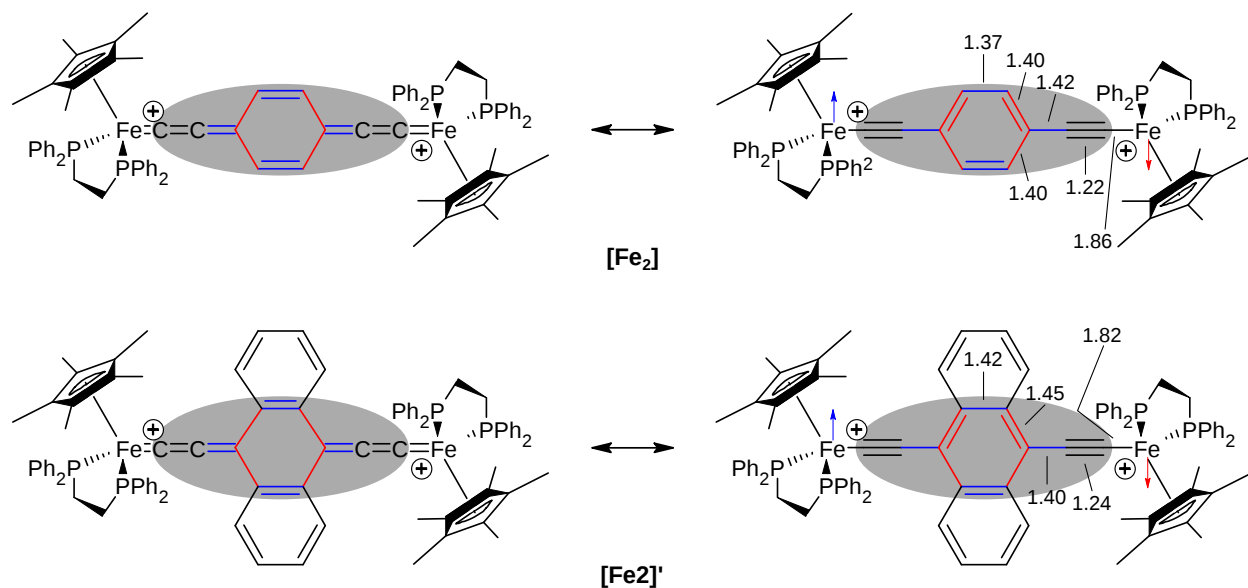


FIG. 4. Lewis structures of $[\text{Fe}_2]$ and $[\text{Fe}_2]'$. The bond lengths (in Å) for $[\text{Fe}_2]$ and $[\text{Fe}_2]'$ are taken from X-ray crystal structures from Ref.⁶¹ and⁶², respectively. Note that the shown structures are, strictly speaking, not resonance structures, since they have different bond lengths. Bonds included in evaluating established BLA measures are shown in red if they were added and in blue if they were subtracted in Eq. (1)^{39,40}. Note that the reference bond lengths within the benzene rings were those of aromatic benzene and not the alternating single and double bonds shown in the Lewis structures. Also, the Fe–C bonds are not included in the evaluation of the structural diradical character, because no reference bond length for Fe–C single and Fe=C double bonds were defined.

structures, which we call structural diradical character, and which is does not directly based on alternating bond lengths, but on comparing each bond length to a reference one from the ideal open-shell or closed-shell structures (see Figure 1 and Section II).

For predicting NLO switching, it is important to not only match the experimental bond length patterns for a given structure, but also to describe trends correctly when changing the bridge. Furthermore, the performance of exchange–correlation functionals may vary due to a dependence of delocalization errors on bridge lengths^{51,63}. Therefore, our goal is to find out, based on our new measure of structural diradical character, whether we can identify a functional that can reproduce bond length patterns for not only organic, but also inorganic compounds, with varied bridges.

We therefore apply this measure to two sets of selected organometallic^{61,62} and organic⁶⁴

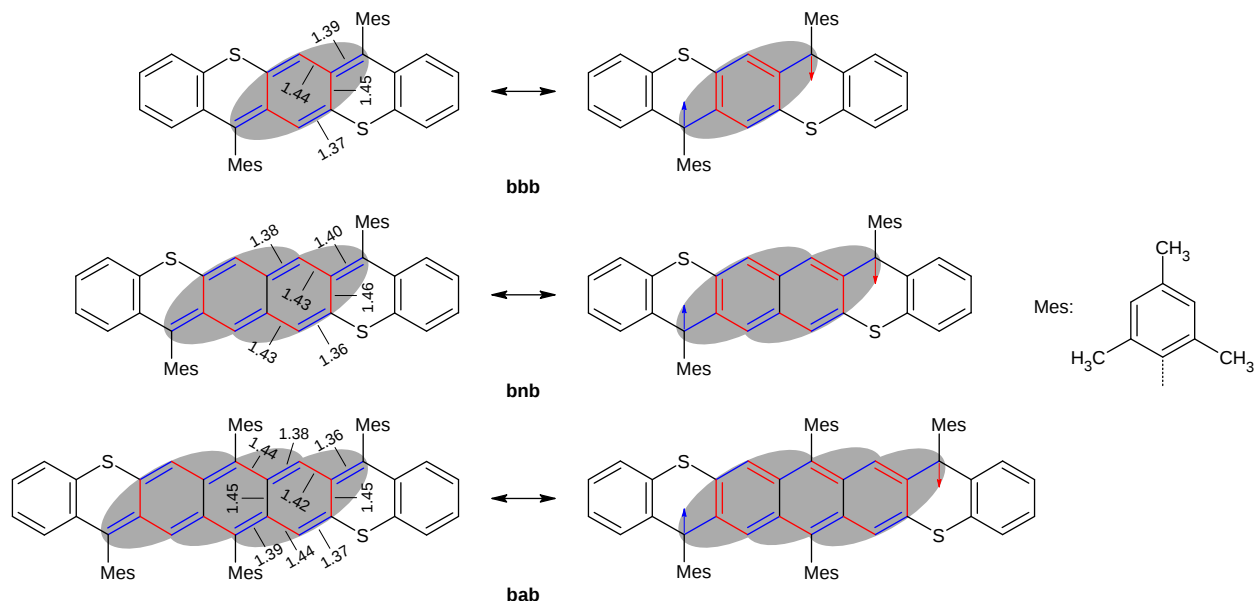


FIG. 5. Lewis structures and selected X-ray crystallographic bond lengths (from Ref.⁶⁴) of **bbb**, **bnb** and **bab**. The closed-shell quinoidal form is shown on the left-hand side, the diradicaloid form on the right-hand side. Note that strictly speaking, these are not mesomeric forms, since bond lengths will differ between the diradicaloid and the closed-shell structures. Bonds included in evaluating established BLA measures are shown in red if they were added and in blue if they were subtracted in Eq. (1)^{39,40}.

reference compounds for which structural data are available from the experiment for given spin centers with two and three different bridges, respectively, and where these variations of the bridge are known to change the diradical character considerably (see Figures 4 and 5). Even though the organometallic systems are quite large molecules, we consider, in contrast to previous work^{61,62}, the full atomistic details of all ligands.

We compare four different exchange–correlation functionals, three of which (BP86, TPSS, TPSSh) have proven valuable for structures and energetics of transition metal complexes^{65–67}, while B3LYP is very popular for open-shell organic molecules. BP86 and TPSS are pure functionals, and TPSSh and B3LYP are hybrid functionals with 10 and 20 percent of exact-exchange admixture, respectively. The pure parts of BP86 and B3LYP are of generalized gradient corrected (GGA) type, and for TPSS and TPSSh, of meta GGA type. Since exact exchange admixture tends to localize spin density^{68–70}, hybrid functionals should favor diradical structures (right-hand side of Figure 1) more strongly than pure ones.

Our measure for *structural* diradical character not only allows to condense comparisons of bond lengths patterns into single numbers, but has the rare property of enabling direct comparisons of diradical character between theory and experiment. In contrast to other such definitions employing *electronic* structure data^{28,71–76}, it shares this property with a definition of diradical character based on experimentally accessible *electronic* properties by Champagne and coworkers⁷⁷.

II. A GENERALLY APPLICABLE STRUCTURAL MEASURE OF DIRADICAL CHARACTER

The studied molecules can be drawn in different forms (see Figures 3 through 5), one of which denotes a closed-shell state (CS) and the other an open-shell state (OS) form bearing two unpaired electrons. These two forms differ in the distribution of C–C bonds (single-, double-, triple- and aromatic bonds) between respective carbon atoms. In the CS, the bond lengths are typically more equally distributed than in the OS.

One way to estimate diradical or open-shell character (we use the two synonymously here) is calculating the BLA defined as the average difference between bonds lengths for N pairs of adjacent bonds ($b_{i,0}$ and $b_{i,1}$),

$$\text{BLA} = \frac{1}{N} \sum_{i=1}^N b_{i,0} - b_{i,1}, \quad (1)$$

which, e.g., can be alternating single and double or alternating single and triple bonds.^{39,40} The bonds that were considered for the BLA are shown in the corresponding figures in red if they were added and in blue if they were subtracted.

Using BLA as a measure for diradical character has some drawbacks. (i) The BLA can only be used for one sort of alternating bonds, while for the iron complexes ($[\text{Fe}_2]$ and $[\text{Fe}_2]'$) there are both alternating single and double bonds, as well as alternating single and triple bonds. One has to choose which set of bonds will be used for calculating the BLA and which will be dismissed. Also, for some inorganic structures such as the tin cluster studied in Ref.⁶⁰, diradical character correlates with the presence or absence of a tin–tin bond rather than bond length alternation. (ii) Pairs of bonds have to be used, meaning that an even number of bonds must be considered. For example, for the biscobaltocenyldithienylethene ($[\text{Co}_2]$) this is not the case, and one has to choose arbitrarily one bond which will not be taken into

account. (iii) The sign of the calculated BLA is choice-dependent and could be switched by adding the bond lengths that were subtracted and vice versa. This indicates that it is difficult to define a unique and transferable measure for diradical character based on bond-length alternation. (iv) The calculated numbers for different systems cannot be directly compared, because the magnitude of the numbers is system-dependent. (v) BLA measures bond length patterns in absolute terms, which implies that when comparing calculated with experimental data, deviations resulting from a general over- or underestimation of bond lengths by a given functional are mixed with those resulting from an inadequate representation of relative bond lengths differences.

This is why we chose to introduce a different measure for estimating the open-shell character (OSC) based on bond lengths. The new measure overcomes the drawbacks of the BLA while still retaining the simplicity of the BLA scheme. It is based on structural similarities with idealized open-shell and closed-shell structures. In order to use the measure for structures obtained from X-ray crystallography and for structures from first-principles optimizations, reference bond lengths for the ideal open-shell and closed-shell structures are employed. For the analysis of X-ray structures, the experimentally determined C–C bond lengths of ethane (single bond), ethene (double bond), ethine (triple bond) and benzene (aromatic bond) are used (taken from Ref⁷⁸).⁷⁹ For calculated structures, bond lengths of the molecules just mentioned, structurally optimized using the same computational settings as for the examined molecule, are employed (see Supplemental Material for details). This implies that in contrast to BLA, a general over- or underestimation of bond lengths by a certain electronic structure method does not affect our desired measure for bond length patterns.

The actual bond lengths b (from X-ray or calculation) are compared to these reference bond lengths b_{ref} , and the normalized mean absolute error ($\text{MAE}_{\text{norm}}^X$; $X = \text{CS}, \text{OS}$),

$$\text{MAE}_{\text{norm}}^X = \frac{\sum_{i=1}^n \frac{|b_i - b_{i,\text{ref}}^X|}{|b_{i,\text{ref}}^{\text{OS}} - b_{i,\text{ref}}^{\text{CS}}|}}{n}, \quad (2)$$

and the normalized root mean squared deviation ($\text{RMSD}_{\text{norm}}^X$; $X = \text{CS}, \text{OS}$),

$$\text{RMSD}_{\text{norm}}^X = \sqrt{\frac{\sum_{i=1}^n \left(\frac{b_i - b_{i,\text{ref}}^X}{|b_{i,\text{ref}}^{\text{OS}} - b_{i,\text{ref}}^{\text{CS}}|} \right)^2}{n}}, \quad (3)$$

are calculated for all n bonds where the reference bond length in the CS and OS differ (these bonds are encapsulated in gray ovals in the corresponding Figures). The normalization is used to account for different magnitudes in reference bond-length differences (20 pm for a C–C \longrightarrow C=C transition, 14 pm for a C=C \longrightarrow C \equiv C transition, 14 pm for a C–C \longrightarrow C=C transition and 6 pm for a C=C \longrightarrow C=C transition).

The structural diradical character y_s is then defined as

$$y_s = 1 - \frac{\text{MAE}_{\text{norm}}^{\text{OS}}}{\text{MAE}_{\text{norm}}^{\text{OS}} + \text{MAE}_{\text{norm}}^{\text{CS}}} = \frac{\text{MAE}_{\text{norm}}^{\text{CS}}}{\text{MAE}_{\text{norm}}^{\text{OS}} + \text{MAE}_{\text{norm}}^{\text{CS}}}. \quad (4)$$

The structural diradical character can be calculated from the $\text{RMSD}_{\text{norm}}^X$ in an analogous way.

A “real-world” closed-shell singlet will by be quite far from a perfect structural diradical character of zero, because π conjugation⁸⁰, chemical substitution, structural distortions and other effects may lead to deviations from ideal bond lengths. For the same reason, what we would clearly consider an open-shell singlet structure will have a y_s smaller than the “perfect” value of one. We may anticipate here that our analysis of selected experimental structures below suggests that structural diradical characters (evaluated from MAEs) around 0.6 indicate the transition between what in the past has typically been considered open-shell and closed-shell singlets.

III. ATTEMPT AT A TRUE FIRST-PRINCIPLES PREDICTION OF DIRADICAL CHARACTER: BISCOBALTOCENYLDITHIENYLETHENE

DTE derivatives can, in principle, be switched from a closed form (Figure 2 left), which has an extended conjugation, to an open form (Figure 2 right), referred to as ring opening, by radiation with visible light. Ring closure (switching from the open form to the closed form) can be initiated by irradiation with UV light (due to a less extended conjugation in the open form). For the closed form with the attached cobaltocenes ($[\text{Co}_2]$), a diradical Lewis structure with two unpaired electrons and a closed-shell structure with no unpaired electrons can be drawn (see Figure 3). It is not known yet experimentally whether the molecule is predominantly OS or CS in its ground state.

In an attempt to make a true first-principles prediction on this question, we have calculated optimized structures (open and closed shell) and analyzed the spin-state energetics

and structural diradical characters of this compound, employing the pure BP86 functional and the hybrid B3LYP with 20 % admixture of Hartree–Fock exchange.

We start molecular structure optimizations for (1) a closed-shell singlet (cs), employing spin-restricted KS DFT (RKS), (2) a broken-symmetry⁸¹ (bs) approximation of the open-shell singlet employing spin-unrestricted KS DFT (UKS), for which the local spin density in the initial guess corresponded to one spin-up unpaired electron on one spin center and one spin-down electron on the other center⁸², and (3) a triplet (t) described by UKS to evaluate singlet–triplet splittings. For a bs solution with approximately one unpaired electron per spin center, a total spin expectation value of $\langle \hat{S}^2 \rangle$ close to one is expected⁸³. The bs approach may converge to a closed-shell solution, which is indicated by $\langle \hat{S}^2 \rangle$ approaching zero. Therefore, $\langle \hat{S}^2 \rangle$ values are reported for all cs and bs optimizations. All molecular structures under study have singlet ground states.

TABLE I. Relative energies with respect to the closed-shell energy (ΔE) [kJ/mol], structural diradical character y_s (Equation 4) (MAE and, in parentheses, RMSD), bond-length alternation (Equation 1) BLA [pm], \hat{S}^2 expectation values ($\langle \hat{S}^2 \rangle$) for the optimized structures of [**Co**₂] (see Figure 3) employing BP86/def2-TZVP and B3LYP/def2-TZVP, for closed-shell (cs), open-shell singlet modeled by a broken-symmetry (bs) determinant, and triplet (t). The structural diradical characters of the energetically most stable structures are highlighted in green (with energies differing by less than 5 kJ/mol considered as degenerate). The overall assignment as closed-shell (CS) or open-shell (OS) is indicated in the right-most column.

| | cs | | | | bs | | | | t | | | |
|----------------------------|--------------|-------------|-----|-----------------------------|------------|-------------|------|-----------------------------|------------|-------------|-------|----|
| | ΔE | y_s | BLA | $\langle \hat{S}^2 \rangle$ | ΔE | y_s | BLA | $\langle \hat{S}^2 \rangle$ | ΔE | y_s | BLA | |
| | BP86 | | | | | | | | | | | |
| [Co ₂] | 0.00 | 0.58 (0.71) | 2.6 | 0.00 | 1.37 | 0.58 (0.71) | 2.6 | 0.01 | 28.45 | 0.67 (0.81) | -1.43 | CS |
| | B3LYP | | | | | | | | | | | |
| [Co ₂] | 0.00 | 0.56 (0.67) | 4.4 | 0.00 | -52.6 | 0.73 (0.87) | -3.4 | 1.10 | 2.04 | 0.74 (0.88) | -3.7 | OS |

For all optimized structures, we evaluate structural diradical character and BLA. If these data agreed reasonably well for the ground-state structures of both BP86 and B3LYP, a DFT prediction of the open-shell character of [**Co**₂] could be considered as reliable. However, BP86 gives a closed-shell structure, while B3LYP results in an open-shell singlet as the

energetically most stable solution (Table I).

The structural diradical character is small for the closed-shell solutions and large for the open-shell solution, which could only be converged with B3LYP, not with BP86, even if performing a single-point calculation on the open-shell optimized B3LYP structure, with the open-shell B3LYP orbitals as initial guess. Interestingly, the BP86 closed-shell singlet shows a larger structural diradical character than the B3LYP one, indicating that even though both are equally closed-shell in terms of electronic structure ($\langle \hat{S}^2 \rangle = 0$), the BP86 molecular structure leans more towards the open-shell side. For comparison, structural diradical character was also evaluated for the triplet. Here, one would expect bond length patterns close to the open-shell resonance structures, and accordingly, y_s is always largest for the triplet. For the B3LYP open-shell singlet, y_s is nearly identical to the value for the triplet, which could be taken as an additional indication that the open-shell-singlet B3LYP solution converges to a nearly pure diradical.

Here, MAE- and RMSD-derived structural diradical characters deviate by up to 0.14, with the latter being larger, while in our reference systems (see below), it does not matter much whether structural diradical character y_s is evaluated with MAE or RMSD as a measure for structural deviations, and the latter is typically slightly smaller. This different behavior might be related to the fact that single / double bond alternation plays a more pronounced role here in *both* structures in contrast to the reference compounds. It makes employing y_s as an absolute measure for diradical character difficult, but as will be discussed below, 0.6 as evaluated based on MAE appears to be a reasonable measure for the transition from what is typically considered more closed-shell to more open-shell singlet, at least for the set of molecules considered here (see also Section 6 in the Supporting Information).

A negative BLA would be expected for an open-shell structure, because the single bonds of the bridge are subtracted (blue in Figure 3) and the double bonds (shorter) are added (red in Figure 3) and the aromatic bonds (same bond lengths in the reference) will not bias the BLA towards positive or negative values. On the other hand, a positive BLA indicates a closed-shell structure, because then the single bonds are added (red in Figure 3), while the double bonds (shorter) are subtracted (blue in Figure 3). The BLA (Equation 1) obtained from the BP86 solutions is small, but positive, rather corresponding to a closed shell, while the BLA obtained from B3LYP is positive for the closed-shell solution and negative for the open-shell solution.

In accordance with the larger open-shell character suggested by B3LYP, the singlet–triplet gap is by more than an order of magnitude smaller than the gap predicted by BP86.

Altogether, these data suggest that according to BP86, $[\text{Co}_2]$ is mostly a closed-shell molecule, while B3LYP suggests it is mostly open-shell. Therefore, in the following we will compare these two exchange-correlation (xc) functionals employed along with two meta-GGA based ones (TPSS and TPSSh) with experimental data on structures where varying the bridge modifies the diradical character.

IV. INORGANIC REFERENCE SYSTEMS: DINUCLEAR CARBON COMPLEXES WITH CARBON-RICH BRIDGES

In the two dicationic complexes shown in Figure 4, two iron(III) centers with one unpaired electron each are linked by carbon-rich bridges, in one case with a benzene linker ($[\text{Fe}_2]$) and in one case with a benzene linker featuring two annelated rings ($[\text{Fe}_2]'$). This annelation should decrease the aromaticity of the central carbon structure, and thus favor the cumulenic structure shown on the left-hand side.

Indeed, in the experiment⁶², analysis of characteristic bond lengths (Fe–C, –C≡C, ≡C–C) of $[\text{Fe}_2]$ revealed a longer Fe–C and ≡C–C and shorter –C≡C bonds as compared to the X-ray structure of $[\text{Fe}_2]'$, indicating a larger structural diradical character. Despite slight differences, this holds for both molecules present in the unit cell (indicated by “xray1” and “xray2” in the lower part of Table II)⁸⁴. Superconducting quantum interference device (SQUID) magnetometry (as powder) revealed a singlet ground state for $[\text{Fe}_2]$ with a thermally accessible triplet state about 4.56 kJ/mol higher in energy, suggesting that the ground state has significant open-shell character. The variable temperature (VT)-UV-Vis spectra did not give any evidence of structural changes between 10 K and 300 K, and VT-IR spectra pointed to a barely detectable increase of cumulenic character with decreasing temperature, suggesting that the structural changes between the singlet and triplet states are minor. Altogether, this was interpreted as $[\text{Fe}_2]$ having significant open-shell singlet character in its ground state, despite the relatively strong antiferromagnetic spin coupling.

For $[\text{Fe}_2]'$, no signal was found in the electron spin resonance (ESR) spectrum at 77 K, so the triplet state is not thermally accessible up to that temperature, corresponding to a singlet–triplet splitting of at least 1200 cm^{-1} (roughly 14.3 kJ/mol). This is also supported

by VT-NMR data. IR spectra support the more cumulenic structure that was also indicated by X-Ray crystallography. This points to $[\mathbf{Fe}_2]'$ having substantial closed-shell character in the ground state.

The y_s data in Table II suggest that hybrid functionals, in particular B3LYP and TPSSh, can describe the structural diradical character of $[\mathbf{Fe}_2]$ very well. For $[\mathbf{Fe}_2]'$, B3LYP overestimates this character somewhat, while TPSSh is very close to the experimental value. Interestingly, the reduction in y_s from $[\mathbf{Fe}_2]$ to $[\mathbf{Fe}_2]'$ is partially described already by the closed-shell-optimized structures. For the open-shell (bs) optimized structures, y_s increases as spins become more localized on the spin centers (as indicated by increasing $\langle \hat{S}^2 \rangle$). This is in line with this localization indicating a stronger importance of the open-shell resonance structure (right-hand side of Figure 4). The B3LYP open-shell-singlet structure for $[\mathbf{Fe}_2]$ has a y_s very close to the value for the triplet, which suggests that B3LYP would consider $[\mathbf{Fe}_2]$ almost purely open shell. For TPSSh, the values are also reasonable close, indicating dominant open-shell character.

Owing to the size of the systems under study (we describe all ligands in full atomistic detail), crystal structure optimizations under periodic boundary conditions (in particular with hybrid functionals) are prohibitively expensive. It has been pointed out that crystal packing can increase quinoidal character⁴³, so our first-principles structural diradical characters for isolated molecules may overestimate the values obtained from X-ray crystallography somewhat. At least for $[\mathbf{Fe}_2]$, measured exchange spin coupling constants were very similar in the solid state and in solution⁶², which suggests that structural differences between the two are not major. Still, it may be that the deviation of B3LYP data from the experiment is partially due to the neglect of packing effects.

Overall, based on the structural diradical character y_s , TPSSh would be considered adequate for describing the two iron-based complexes under study here (with B3LYP being also acceptable). TPSSh also matches the experimental singlet–triplet energy splitting for $[\mathbf{Fe}_2]$ quite nicely (2.9 kJ/mol vs. 4.56 kJ/mol), and is not too far from the experimental lower bound on this splitting for $[\mathbf{Fe}_2]'$ (8.1 kJ/mol vs. 14.3 kJ/mol), whereas B3LYP underestimates both.

TABLE II. Relative energies with respect to the closed-shell energy (ΔE) [kJ/mol], structural diradical character y_s (Equation 4) (MAE and, in parentheses, RMSD), bond-length alternation (Equation 1) BLA [pm], \hat{S}^2 expectation values ($\langle \hat{S}^2 \rangle$) for the optimized structures of $[\text{Fe}_2]$ and $[\text{Fe}_2]'$ (see Figure 4) for closed-shell (cs), open-shell singlet modeled by a broken-symmetry (bs) determinant, and triplet (t), and available data for the X-ray structures (with the two molecules present in the unit cell (indicated by “xray1” “and xray2”). For an explanation of the error estimation of the y_s and BLA values see Supplemental Material. The structural diradical characters of the energetically most stable structures are highlighted in green (with energies differing by less than 5 kJ/mol considered as degenerate). The overall assignment based on experimental data^{61,62} as closed-shell (CS) or open-shell (OS) is also indicated in the bottom left cells.

| | cs | | | | bs | | | | t | | | |
|--------------------------------|--|-------------|------|-----------------------------|------------|---------------|-------------|-----------------------------|------------|-------------|-------|--|
| | ΔE | y_s | BLA | $\langle \hat{S}^2 \rangle$ | ΔE | y_s | BLA | $\langle \hat{S}^2 \rangle$ | ΔE | y_s | BLA | |
| | BP86 | | | | | | | | | | | |
| $[\text{Fe}_2]$ | 0.00 | 0.56 (0.56) | 6.0 | 0.00 | -4.45 | 0.63 (0.62) | 4.2 | 0.62 | 5.76 | 0.71 (0.68) | 2.25 | |
| $[\text{Fe}_2]'$ | 0.00 | 0.46 (0.46) | 5.7 | 0.00 | 0.00 | 0.46 (0.46) | 5.7 | 0.00 | 26.7 | 0.60 (0.59) | 1.55 | |
| | TPSS | | | | | | | | | | | |
| $[\text{Fe}_2]$ | 0.00 | 0.57 (0.56) | 5.85 | 0.00 | -9.87 | 0.66 (0.65) | 3.4 | 0.81 | -1.54 | 0.72 (0.70) | 1.8 | |
| $[\text{Fe}_2]'$ | 0.00 | 0.45 (0.45) | 5.5 | 0.00 | -0.338 | 0.47 (0.47) | 4.9 | 0.25 | 22.3 | 0.63 (0.62) | 1.0 | |
| | TPSSh | | | | | | | | | | | |
| $[\text{Fe}_2]$ | 0.00 | 0.55 (0.55) | 6.3 | 0.00 | -50.1 | 0.73 (0.71) ✓ | 1.5 | 1.06 | -47.2 | 0.77 (0.73) | 0.85 | |
| $[\text{Fe}_2]'$ | 0.00 | 0.45 (0.45) | 6.0 | 0.00 | -19.0 | 0.61 (0.60) ✓ | 1.8 | 1.04 | -10.9 | 0.71 (0.68) | -0.22 | |
| | B3LYP | | | | | | | | | | | |
| $[\text{Fe}_2]$ | 0.00 | 0.54 (0.53) | 6.9 | 0.00 | -101 | 0.78 (0.74) ✓ | 0.7 | 1.11 | -100 | 0.79 (0.75) | 0.4 | |
| $[\text{Fe}_2]'$ | 0.00 | 0.44 (0.44) | 6.6 | 0.00 | -62.9 | 0.68 (0.67) | -0.1 | 1.14 | -60.2 | 0.74 (0.71) | -0.85 | |
| | X-ray^{61,62} | | | | | | | | | | | |
| | y_s | | | | | | BLA | | | | | |
| $[\text{Fe}_2]_{\text{xray1}}$ | 0.76 ± 0.03 (0.71 ± 0.03) OS | | | | | | 0.20 ± 0.80 | | | | | |
| $[\text{Fe}_2]_{\text{xray2}}$ | 0.78 ± 0.03 (0.72 ± 0.02) OS | | | | | | 0.20 ± 0.80 | | | | | |
| $[\text{Fe}_2]'$ | 0.59 ± 0.03 (0.58 ± 0.03) CS (with some OS?) | | | | | | 3.90 ± 0.40 | | | | | |

With bond-length alternation, it is more difficult to obtain a clear picture. Bond-length alternation should be more pronounced for the more quinoidal form of $[\mathbf{Fe}_2]'$ compared with $[\mathbf{Fe}_2]$, and this is indeed the case for the structures obtained from experiment. Also, the BLA of an open-shell solution (if one is converged) is, as expected, smaller than for a closed-shell solution. For the DFT-optimized structures, BLA data vary significantly depending on the xc functional employed. The increase in BLA from $[\mathbf{Fe}_2]$ to $[\mathbf{Fe}_2]'$ is only reproduced for the two pure functionals (for which attempts at broken-symmetry optimizations converge to $\langle \hat{S}^2 \rangle$ smaller than one), and in terms of absolute numbers, there is no functional which agrees well with the BLA for both $[\mathbf{Fe}_2]$ and $[\mathbf{Fe}_2]'$. For $[\mathbf{Fe}_2]$, B3LYP comes closest (but fails for $[\mathbf{Fe}_2]'$), and for $[\mathbf{Fe}_2]'$, TPSS matches best (but strongly overestimates BLA for $[\mathbf{Fe}_2]$). Also, while y_s changes only slightly when varying bond lengths within the experimental error bar (see Supplemental Material for details), these variations affect BLA values considerably. All this suggests that in contrast to y_s , it is at least difficult to identify a reliable xc functional for structural diradical character based on BLA.

V. ORGANIC REFERENCE SYSTEMS: BISBENZOTHIAQUINODIMETHANES WITH VARYING BRIDGE LENGTHS

Bisbenzothiaquinodimethanes (see Figure 5) have recently been presented as stable analogues of larger acenes, enabling the experimental study of diradical character as a function of molecular length⁶⁴. While all three molecules under study showed considerable quinoidal character, diradical character increased with increasing molecular length as expected, owing to the increasing number of aromatic rings formed in the open-shell resonance structure⁸⁵. This was concluded, among others, from the X-Ray crystallographic structures and from the increased spectral broadening in VT ¹H-NMR, indicating more strongly thermally populated triplet states for longer molecules.

We optimized the molecular structures in the closed-shell, open-shell singlet (bs), and triplet states with the four xc functionals under consideration (see Table III). Here, we employed Grimme’s empirical dispersion correction (D3)⁸⁶, since it has been proven important for extended organic systems. We had not employed this correction for the inorganic complexes above, because its suitability for inorganic systems is not as clearly established as for

organic ones⁶⁷.

For all functionals and structures, we obtain either a closed-shell solution as the ground state, or an open-shell singlet (bs) that is close in energy to the closed-shell one. The energy differences between the two are at most around 3.5 kJ/mol, which appears too close to the DFT error margin to make a well-founded decision on which of the two represents the ground state better. The \hat{S}^2 expectation values of the bs solutions are often close to zero and never larger than about 0.6, indicating partial closed-shell character. The larger $\langle \hat{S}^2 \rangle$, the more the structural diradical characters y_s and bond-length alternation deviate from the “true” closed-shell solution. In all cases, the triplets are considerably higher in energy, consistent with the dominantly closed-shell ground states, and the singlet–triplet splitting of 27 kJ/mol obtained from B3LYP-D3 is consistent with the 22 kJ/mol obtained from temperature-dependent magnetic susceptibility measurements of the **bab** powder and with the 23 kJ/mol obtained previously from UCAM-B3LYP/6-31G(d,p)⁶⁴. This is also in line with the singlet y_s always being considerably lower than the triplet values, suggesting that no singlet has bond length patterns corresponding to pure open-shell structures.

The structural diradical characters y_s for the B3LYP-D3 closed-shell solutions match the experiment almost perfectly. For the longest molecule **bab**, the bs optimization converges to structures with a $\langle \hat{S}^2 \rangle$ value of roughly 0.6, which is slightly lower in energy and features a larger y_s than the cs solution (0.71 vs. 0.63). Given the quite small energy differences, this bs solution may be an artifact of DFT. It could also be that the good match of the cs data results from an error compensation between the electronic structure description and the neglect of crystal packing effects (compare the discussion in the preceding section). Without the experimental reference, there would be little solid criteria for deciding which of the two describes the experiment better.

As exact exchange admixtures increase in the functionals, the structural diradical characters of the closed-shell solutions increase slightly, leading to an overestimation of the experimental values (that could still be consistent with the experiment if packing effects should play a role).

TABLE III. Relative energies with respect to the closed-shell energy (ΔE) [kJ/mol], structural diradical character y_s (Equation 4) (MAE and, in parentheses, RMSD), bond-length alternation (Equation 1) BLA [pm], \hat{S}^2 expectation values ($\langle \hat{S}^2 \rangle$) for the optimized structures of **bbb**, **bnb** and **bab** (see Figure 5) for closed-shell (cs), open-shell singlet modeled by a broken-symmetry (bs) determinant, and triplet (t), and available data for the X-ray structures. For an explanation of the error estimation of the y_s and BLA values see Supplemental Material. The structural diradical characters of the energetically most stable structures are highlighted in green (with energies differing by less than 5 kJ/mol considered as degenerate). The overall assignment based on experimental data^{61,62} as closed-shell (CS) or open-shell (OS) is also indicated in the bottom left cells.

| | cs | | | | bs | | | | t | | |
|------------|---|---------------|-----|-----------------------------|------------|---------------|-------------|-----------------------------|------------|-------------|-------|
| | ΔE | y_s | BLA | $\langle \hat{S}^2 \rangle$ | ΔE | y_s | BLA | $\langle \hat{S}^2 \rangle$ | ΔE | y_s | BLA |
| | BP86-D3 | | | | | | | | | | |
| bbb | 0.00 | 0.57 (0.56) | 5.8 | 0.00 | -0.137 | 0.57 (0.56) | 5.8 | 0.000 | 80.9 | 0.79 (0.76) | 0.05 |
| bnb | 0.00 | 0.65 (0.64) | 4.9 | 0.00 | 0.101 | 0.65 (0.64) | 4.9 | 0.000 | 55.5 | 0.78 (0.76) | 1.05 |
| bab | 0.00 | 0.69 (0.67) | 4.5 | 0.00 | 0.180 | 0.69 (0.67) | 4.4 | 0.001 | 39.5 | 0.77 (0.75) | 1.44 |
| | TPSS-D3 | | | | | | | | | | |
| bbb | 0.00 | 0.56 (0.56) | 5.9 | 0.00 | -0.035 | 0.54 (0.53) | 6.5 | 0.000 | 78.4 | 0.80 (0.77) | -0.35 |
| bnb | 0.00 | 0.65 (0.64) | 5.1 | 0.00 | 0.156 | 0.66 (0.64) | 5.0 | 0.001 | 52.1 | 0.78 (0.76) | 0.88 |
| bab | 0.00 | 0.69 (0.67) | 4.5 | 0.00 | 0.138 | 0.70 (0.67) | 4.4 | 0.031 | 35.6 | 0.76 (0.75) | 1.2 |
| | TPSSh-D3 | | | | | | | | | | |
| bbb | 0.00 | 0.54 (0.54) | 6.5 | 0.00 | -0.111 | 0.54 (0.54) | 6.5 | 0.000 | 73.6 | 0.81 (0.78) | -0.75 |
| bnb | 0.00 | 0.65 (0.64) | 5.1 | 0.00 | 0.172 | 0.63 (0.62) ✓ | 5.4 | 0.074 | 43.9 | 0.79 (0.76) | 0.67 |
| bab | 0.00 | 0.66 (0.64) ✓ | 5.1 | 0.00 | -2.21 | 0.72 (0.69) | 3.8 | 0.516 | 25.4 | 0.77 (0.75) | 1.06 |
| | B3LYP-D3 | | | | | | | | | | |
| bbb | 0.00 | 0.51 (0.51) ✓ | 7.4 | 0.00 | -0.152 | 0.51 (0.51) ✓ | 7.3 | 0.000 | 75.2 | 0.81 (0.77) | -0.63 |
| bnb | 0.00 | 0.59 (0.58) ✓ | 6.5 | 0.00 | 0.115 | 0.60 (0.59) ✓ | 6.2 | 0.109 | 43.3 | 0.78 (0.76) | 0.83 |
| bab | 0.00 | 0.63 (0.62) ✓ | 6.0 | 0.00 | -3.46 | 0.71 (0.68) | 4.2 | 0.594 | 23.5 | 0.77 (0.75) | 1.3 |
| | X-ray⁶⁴ | | | | | | | | | | |
| | y_s | | | | | | BLA | | | | |
| bbb | 0.50 ± 0.02 (0.50 ± 0.02) CS | | | | | | 6.85 ± 0.26 | | | | |
| bnb | 0.59 ± 0.01 (0.58 ± 0.01) CS (with some OS) | | | | | | 5.93 ± 0.40 | | | | |
| bab | 0.63 ± 0.02 (0.62 ± 0.02) CS (with some OS) | | | | | | 5.55 ± 0.34 | | | | |

Bond length alternation decreases as the molecules get longer, which is consistent with the increasing diradical character. Also if BLA is taken as a criterion, closed-shell B3LYP-D3 matches the experiment well, slightly overestimating BLA, while TPSSh errs in the other direction showing the best agreement of the functionals considered. For these organic systems, BLA is much more consistent over different functionals, and the conclusions drawn from BLA and y_s are similar: the two hybrid functionals are suited best to describe bond length patterns in these organic diradical candidates. This good agreement between the two measures may be because (1) BLA is more suitable for organic systems than for inorganic ones, and because (2) the same sets of bonds are employed in evaluating these measures here, in contrast to the diiron and dicobalt complexes discussed above. Furthermore, while experimental error bars on bond lengths still affect BLA values more than y_s , this is much less severe than it was the case for the two diiron complexes discussed above, so for organic systems, both BLA and y_s appear as reasonable choices for evaluating agreement between calculated and experimental bond length patterns.

VI. CONCLUSION

For predicting nonlinear optical properties of molecules, it is essential to provide correct bond lengths patterns based on first-principles electronic structure methods. While bond-length alternation (BLA) works as an adequate measure for comparing calculated with experimental molecular structures, we found that it fails for two organometallic diiron complexes in which the aromaticity of a carbon-rich bridge strongly influences diradical character. This is because BLA is not uniquely defined for these structures, leaves out essential bonds, and provides values which scatter unsystematically when comparing different exchange–correlation functionals within Kohn–Sham density functional theory.

We have therefore suggested a new measure, structural diradical character y_s , which is based on comparisons between molecular structures and idealized closed-shell and diradical structures. We can show that with this new measure, consistent comparisons between experiment and first-principles molecular structures are possible.

Based on these comparisons, we can identify two hybrid functionals, TPSSh and B3LYP, with 10 and 20 percent of exact exchange admixture, as suitable for describing structural diradical character in both organic and organometallic systems. B3LYP (with Grimme’s

empirical dispersion corrections) works best for the organic molecules, and TPSSh (without dispersion correction) for the organometallic complexes under study. Importantly, these functionals were also the ones which gave a realistic description of singlet–triplet energy differences. The GGA and meta-GGA functionals BP86 and TPSS turned out not suitable for neither purpose.

The excellent agreement for B3LYP-D3 was only found when the organic molecules (a series of bisbenzothiaquinodimethanes with different molecular lengths) were described as closed-shell electronic structures (restricted KS-DFT), even though in some cases broken-symmetry solutions with partial open-shell singlet character were slightly lower in energy, but within typical DFT error bars (up to 3.5 kJ/mol). This illustrates that present-day KS DFT may be unable to make predictions in cases like these, where closed-shell and open-shell singlets are close in energy. On the upside, there exists one frequently used functional, B3LYP, which is able to provide perfect agreement for these structures when only the closed-shell singlets are considered. Possibly, these data could indicate that when singlet–triplet gaps are large, and when closed- and open-shell singlets are nearly degenerate, one should consider the closed-shell singlets as more reliable for present-day standard xc functionals. However, such statements clearly require more research, possibly also considering schemes which combine a more explicit description of static correlation with Kohn–Sham DFT^{87–91}.

Comparing structural diradical character y_s obtained from experiment with assignments as (predominantly) open-shell or closed-shell from the literature suggests that y_s smaller than roughly 0.6 (with MAE as a measure for structural deviations) points to a more closed-shell structure, while larger y_s correspond to more open-shell structures. Closeness to triplet y_s values may also serve as an absolute criterion for pure open-shell character (usually only applicable to computed structures, however). For closed-shell electronic structures, y_s slightly decreases with increasing exact exchange admixture, while for open-shell singlet, it increases, so that differences between the two structures become more pronounced.

Our work was motivated by our attempt at a true first-principles prediction of the open-shell character for a photoswitchable [Co₂] complex, which may be a structure worth pursuing and optimizing further for achieving photoswitchable NLO properties. Our findings imply that B3LYP, which suggests an open-shell singlet ground state, is more reliable than BP86, which favors the closed-shell singlet. Therefore, further research into this and related compounds, and their switchability, appears a worthwhile avenue of research.

VII. APPENDIX: THEORETICAL METHODS

All electronic structure calculations were performed using the TURBOMOLE 6.5 program package imposing no symmetry (C_1 symmetry) on the systems. A value of 10^{-7} a.u. was set as the convergence criterion for the energy during self-consistent field calculations. For the molecular structure optimizations the threshold was set to 10^{-6} a.u. for the energy change, to 10^{-3} a.u. for the maximum displacement element, to 10^{-4} a.u. for the maximum gradient element, to $5 \cdot 10^{-4}$ a.u. for the root mean square of the displacement, and to $5 \cdot 10^{-4}$ a.u. for the root mean square of the gradient. The employed xc functional (either BP86^{92,93}, TPSS⁹⁴, TPSSH^{95,96} or B3LYP⁹⁷⁻⁹⁹) and basis set (either def-TZVP^{100,101} or def2-TZVP^{102,103}) and whether the third generation empirical dispersion correction of Grimme (D3)¹⁰⁴ was used or not is indicated in the respective tables.

For the closed-shell calculations restricted KS-DFT was employed. In order to obtain the broken-symmetry determinants, an unrestricted KS-DFT calculation of the triplet state was performed and followed by a subsequent broken-symmetry calculation using Turbomole’s “flip” option on the triplet determinant for obtaining the initial guess for the broken-symmetry calculation. The calculated ground state was then determined by comparison of the energies of the determinants and their corresponding $\langle \hat{S}^2 \rangle$ values. A closed-shell determinant will always have a $\langle \hat{S}^2 \rangle$ value of zero, while in an open-shell determinant representing a diradicaloid there will be a $\langle \hat{S}^2 \rangle$ value larger than zero. This is referred to as spin contamination. For discussions on the validity of broken-symmetry energies, see, e.g., Refs.¹⁰⁵⁻¹¹³. On the one hand, it is argued that the Kohn–Sham reference system of noninteracting fermions should have the same $\langle \hat{S}^2 \rangle$ value as the real, interacting system, and following this argument, schemes have been suggested for estimating the molecular structure of the spin-projected open-shell singlet based on broken–symmetry calculations¹¹⁴. On the other hand, it is not generally established how to evaluate the $\langle \hat{S}^2 \rangle$ value of the interacting system in Kohn–Sham DFT, and there is no unique established way for handling possible double counting of electron correlation when employing spin projection on top of broken-symmetry Kohn–Sham determinants⁸⁷⁻⁹⁰. In practice, the Broken-Symmetry approach has been very successful in modeling molecular structures and energetics of antiferromagnetically coupled systems^{70,105}. We take a pragmatic approach here, directly evaluating the broken-symmetry energies as those of the open-shell singlet.

VIII. ACKNOWLEDGMENT

The authors acknowledge funding by the German Research Foundation (DFG) via SFB 668, the high-performance-computing team of the Regional Computer Center at University of Hamburg and the North-German Supercomputing Alliance (HLRN) for technical support and computational resources. The authors thank Markus Reiher, ETH Zurich, and Jürgen Heck, University of Hamburg, for valuable discussions.

REFERENCES

- ¹M. Abe, *Chem. Rev.* **113**, 7011 (2013).
- ²T. Enoki and T. Ando, *Physics and chemistry of graphene: graphene to nanographene* (CRC Press, 2013).
- ³C. Lambert, *Angew. Chem. Int. Ed.* **50**, 1756 (2011).
- ⁴Z. Sun, Q. Ye, C. Chi, and J. Wu, *Chem. Soc. Rev.* **41**, 7857 (2012).
- ⁵Y. Jung and M. Head-Gordon, *J. Phys. Chem. A* **107**, 7475 (2003).
- ⁶J. Michl, *J. Am. Chem. Soc.* **118**, 3568 (1996).
- ⁷L. Salem and C. Rowland, *Angew. Chem., Int. Ed.* **11**, 92 (1972).
- ⁸W. C. Lineberger and W. T. Borden, *Phys. Chem. Chem. Phys.* **13**, 11792 (2011).
- ⁹J. M. Lenhardt, M. T. Ong, R. Choe, C. R. Evenhuis, T. J. Martinez, and S. L. Craig, *Science* **329**, 1057 (2010).
- ¹⁰T. Stuyver, S. Fias, F. D. Proft, P. Geerlings, Y. Tsuji, and R. Hoffmann, *J. Chem. Phys.* **146**, 092310 (2017).
- ¹¹M. Nakano and B. Champagne, *J. Chem. Phys.* **138**, 244306 (2013).
- ¹²K. D. Nanda and A. I. Krylov, *J. Chem. Phys.* **146**, 224103 (2017).
- ¹³S. Muhammad, M. Nakano, A. G. Al-Sehemi, Y. Kitagawa, A. Irfan, A. R. Chaudhry, R. Kishi, S. Ito, K. Yoneda, and K. Fukuda, *Nanoscale* **8**, 17998 (2016).
- ¹⁴F. Castet, V. Rodriguez, J.-L. Pozzo, L. Ducasse, A. Plaquet, and B. Champagne, *Acc. Chem. Res.* **46**, 2656 (2013).
- ¹⁵P. Beaujean, F. Bondu, A. Plaquet, J. Garcia-Amorós, J. Cusido, F. M. Raymo, F. Castet, V. Rodriguez, and B. Champagne, *J. Am. Chem. Soc.* **138**, 5052 (2016).
- ¹⁶Z. Sun, T. Chen, X. Liu, M. Hong, and J. Luo, *J. Am. Chem. Soc.* **137**, 15660 (2015).

- ¹⁷S. Attar, D. Espa, F. Artizzu, L. Pilia, A. Serpe, M. Pizzotti, G. D. Carlo, L. Marchio, and P. Deplano, *Inorg. Chem.* **56**, 6763 (2017).
- ¹⁸E. Cariati, X. Liu, Y. Geng, A. Forni, E. Lucenti, S. Righetto, S. Decurtins, and S.-X. Liu, *Phys. Chem. Chem. Phys.* **19**, 22573 (2017).
- ¹⁹M. Schulze, M. Utecht, T. Moldt, D. Przyrembel, C. Gahl, M. Weinelt, P. Saalfrank, and P. Tegeder, *Phys. Chem. Chem. Phys.* **17**, 18079 (2015).
- ²⁰K. Okuno, Y. Shigeta, R. Kishi, and M. Nakano, *J. Phys. Chem. Lett.* **4**, 2418 (2013).
- ²¹M. Torrent-Sucarrat, S. Navarro, E. Marcos, J. M. Anglada, and J. M. Luis, *J. Phys. Chem. C* **121**, 19348 (2017).
- ²²P. R. Florindo, P. J. Costa, M. F. M. Piedade, and M. P. Robalo, *Inorg. Chem.* **56**, 6849 (2017).
- ²³M. Nakano and B. Champagne, *Wiley Interdiscip. Rev. Comput. Mol. Sci.* **6**, 198 (2016).
- ²⁴S. Bonness, E. Botek, and B. Champagne, *J. Chem. Phys.* **132**, 094107 (2010).
- ²⁵Y. Inoue, T. Yamada, B. Champagne, and M. Nakano, *Chem. Phys. Lett.* **570**, 75 (2013).
- ²⁶T. Yamada, S. Takamuku, H. Matsui, B. Champagne, and M. Nakano, *Chem. Phys. Lett.* **608**, 68 (2014).
- ²⁷K. Hatua and P. K. Nandi, *Chem. Phys. Lett.* **628**, 1 (2015).
- ²⁸M. Nakano, R. Kishi, T. Nitta, T. Kubo, K. Nakasuji, K. Kamada, K. Ohta, B. Champagne, E. Botek, and K. Yamaguchi, *J. Phys. Chem. A* **109**, 885 (2005).
- ²⁹F. D. Vila, D. A. Strubbe, Y. Takimoto, X. Andrade, A. Rubio, S. G. Louie, and J. J. Rehr, *J. Chem. Phys.* **133**, 034111 (2010).
- ³⁰T. Seidler, K. Stadnicka, and B. Champagne, *J. Chem. Theory Comput.* **10**, 2114 (2014).
- ³¹C. D. Sherrill, E. T. Seidl, and H. F. Schaefer III, *J. Phys. Chem.* **96**, 37123716 (1992).
- ³²M. P. Bahlke, M. Karolak, and C. Herrmann, *Phys. Rev. B* **97**, 035119 (2018).
- ³³S. L. Skornyakov, V. I. Anisimov, D. Vollhardt, and I. Leonov, *Phys. Rev. B* **96**, 035137 (2017).
- ³⁴M. Plihal and D. C. Langreth, *Phys. Rev. B* **58**, 2191 (1998).
- ³⁵K. Matsuda and M. Irie, *Tetrahedron Lett.* **41**, 2577 (2000).
- ³⁶S. H. Kawai, S. L. Gilat, and J.-M. Lehn, *Chem. Commun.* , 1011 (1994).
- ³⁷A. Escribano, T. Steenbock, C. Stork, C. Herrmann, and J. Heck, *ChemPhysChem* **18**, 596 (2017).
- ³⁸K. Matsuda and M. Irie, *J. Am. Chem. Soc.* **122**, 7195 (2000).

- ³⁹W. A. Chalifoux, R. McDonald, M. J. Ferguson, and R. R. Tykwinski, *Angew. Chem. Int. Ed.* **48**, 7915 (2009).
- ⁴⁰E. J. Bylaska, J. H. Weare, and R. Kawai, *Phys. Rev. B* **58**, R7488 (1998).
- ⁴¹S. Shil and C. Herrmann, *J. Comput. Chem.* (2018), accepted, DOI 10.1002/jcc.25153.
- ⁴²S. Nenon and B. Champagne, *J. Chem. Phys.* **138**, 204107 (2013).
- ⁴³T. Seidler, K. Stadnicka, and B. Champagne, *J. Chem. Phys.* **139**, 114105 (2013).
- ⁴⁴B. Champagne, E. A. Perpete, D. Jacquemin, S. J. A. van Gisbergen, E.-J. Baerends, C. Soubra-Ghaoui, K. A. Robins, and B. Kirtman, *J. Phys. Chem. A* **104**, 4755 (2000).
- ⁴⁵F. A. Bulat, A. Toro-Labbe, B. Champagne, B. Kirtman, and W. Yang, *J. Chem. Phys.* **123**, 014319 (2005).
- ⁴⁶H. Sekino, Y. Maeda, M. Kamiya, and K. Hirao, *J. Chem. Phys.* **126**, 014107 (2007).
- ⁴⁷D. Jacquemin, E. A. Perpete, M. Medved, G. Scalmani, M. J. Frisch, R. Kobayashi, and C. Adamo, *J. Chem. Phys.* **126**, 191108 (2007).
- ⁴⁸K. Y. Saponitsky, S. Tafur, and A. E. Masunov, *J. Chem. Phys.* **129**, 044109 (2008).
- ⁴⁹S. Borini, Limacher, P. A., and H. P. Luthi, *J. Chem. Phys.* **131**, 124105 (2009).
- ⁵⁰P. Karamanis, R. Marchal, P. Carbonniere, and C. Pouchan, *J. Chem. Phys.* **135**, 044511 (2011).
- ⁵¹H. Sun and J. Autschbach, *ChemPhysChem* **14**, 2450 (2013).
- ⁵²K. Garrett, X. S. Vazquez, S. B. Egri, J. Wilmer, L. E. Johnson, B. H. Robinson, and C. M. Isborn, *J. Chem. Theory Comput.* **10**, 3821 (2014).
- ⁵³A. J. Garza, O. I. Osman, A. M. Asiri, and G. E. Scuseria, *J. Phys. Chem. B* **119**, 1202 (2015).
- ⁵⁴C. Wang, Y. Yuan, and X. Tian, *J. Comput. Chem.* **38**, 594 (2017).
- ⁵⁵R. Kishi, S. Bonness, K. Yoneda, H. Takahashi, M. Nakano, E. Botek, B. C. T. Kubo, K. Kamada, K. Ohta, and T. Tsuneda, *J. Chem. Phys.* **132**, 094107 (2010).
- ⁵⁶M. Büchert, T. Steenbock, C. Lukaschek, M. C. Wolff, C. Herrmann, and J. Heck, *Chem. Eur. J.* **20**, 14351 (2014).
- ⁵⁷A. Ye, S. Patchkovskii, and J. Autschbach, *J. Chem. Phys.* **127**, 074104 (2007).
- ⁵⁸A. Ye and J. Autschbach, *J. Chem. Phys.* **125**, 234101 (2006).
- ⁵⁹S. Bock, S. G. Eaves, M. Parthey, M. Kaupp, B. L. Guennic, J.-F. Halet, D. S. Yufit, J. A. K. Howard, and P. J. Low, *Dalton Trans.* **42**, 4240 (2013).
- ⁶⁰C. Schrenk, A. Kubas, K. Fink, and A. Schnepf, *Angew. Chem. Int. Ed.* **50**, 7273 (2011).

- ⁶¹F. de Montigny, G. Argouarch, K. Costuas, J.-F. Halet, T. Roisnel, L. Toupet, and C. Lapinte, *Organometallics* **24**, 4558 (2005).
- ⁶²F. Paul, A. Bondon, G. da Costa, F. Malvolti, S. Sinbandhit, O. Cador, K. Costuas, L. Toupet, and M.-L. Boillot, *Inorg. Chem.* **48**, 10608 (2009).
- ⁶³S. R. Whittleton, X. A. S. Vazquez, C. M. Isborn, and E. R. Johnson, *J. Chem. Phys.* **142**, 184106 (2015).
- ⁶⁴S. Dong, T. S. Heng, T. Y. Gopalakrishna, H. Phan, Z. L. Lim, P. Hu, R. D. Webster, J. Ding, and C. Chi, *Angew. Chem.* **128**, 9462 (2016).
- ⁶⁵F. Furche and J. P. Perdew, *J. Chem. Phys.* **124**, 044103 (2006).
- ⁶⁶M. P. Waller, H. Braun, N. Hojdis, and M. Bühl, *J. Chem. Theory Comput.* **3**, 2234 (2007).
- ⁶⁷T. Weymuth, E. P. A. Couzijn, P. Chen, and M. Reiher, *J. Chem. Theory Comput.* **10**, 3092 (2014).
- ⁶⁸C. Herrmann, M. Reiher, and B. A. Hess, *J. Chem. Phys.* **122**, 034102 (2005).
- ⁶⁹C. Herrmann, L. Yu, and M. Reiher, *J. Comput. Chem.* **27**, 1223 (2006).
- ⁷⁰C. J. Cramer and D. G. Truhlar, *Phys. Chem. Chem. Phys.* **11**, 10757 (2009).
- ⁷¹M. Nakano, K. Fukuda, S. Ito, H. Matsui, T. Nagami, S. Takamuku, Y. Kitagawa, and B. Champagne, *J. Phys. Chem. A* **121**, 861 (2017).
- ⁷²E. Ramos-Cordoba and P. Salvador, *Phys. Chem. Chem. Phys.* **16**, 9565 (2014).
- ⁷³V. Bachler, G. Olbrich, F. Neese, and K. Wieghardt, *Inorg. Chem.* **41**, 4179 (2002).
- ⁷⁴D. Herebian, K. E. Wieghardt, and F. Neese, *J. Am. Chem. Soc.* **125**, 10997 (2003).
- ⁷⁵B. Braida, S. E. Galembeck, and P. C. Hiberty, *J. Chem. Theory Comput.* **13**, 3228 (2017).
- ⁷⁶F. Neese, *J. Phys. Chem. Sol.* **65**, 781 (2004).
- ⁷⁷K. Kamada, K. Ohta, A. Shimizu, T. Kubo, R. Kishi, H. Takahashi, E. Botek, B. Champagne, and M. Nakano, *J. Phys. Chem. Lett.* **1**, 937 (2010).
- ⁷⁸W. M. Haynes, *CRC Handbook of Chemistry and Physics, 97th Edition* - (CRC Press, Boca Raton, Fla, 2016).
- ⁷⁹For structures such as the tin cluster referred to above⁶⁰, one could define reference bond lengths for typical tin–tin single bonds for the closed-shell and the sum of two tin van-der-Waals radii for the open-shell structure. This structure would clearly be a challenge for structural measures of diradical character.

- ⁸⁰N. C. Craig, P. Groner, and D. C. McKean, *J. Phys. Chem. A* **110**, 7461 (2006).
- ⁸¹L. Noodleman, *J. Chem. Phys.* **74**, 5737 (1981).
- ⁸²“Spin center” refers to the metal atoms in the organometallic complexes, and to the formally spin-bearing carbon atoms in the diradical resonance structure for the organic structures.
- ⁸³A. Szabo and N. S. Ostlund, *Modern Quantum Chemistry: Introduction to Advanced Electronic Structure Theory* (Dover Publications, New York, 1996).
- ⁸⁴Interpolated data between the two structures can be found in the Supporting Information.
- ⁸⁵G. Trinquier and J.-P. Malrieu, *Chem. Eur. J.* **21**, 814 (2016).
- ⁸⁶S. Grimme, *Wiley Interdiscip. Rev. Comput. Mol. Sci.* **1**, 211 (2011).
- ⁸⁷G. Li Manni, R. K. Carlson, S. Luo, D. Ma, J. Olsen, D. G. Truhlar, and L. Gagliardi, *J. Chem. Theory Comput.* **10**, 3669 (2014).
- ⁸⁸M. Hubert, E. D. Hedegard, and H. J. A. Jensen, *J. Chem. Theory Comput.* **12**, 2203 (2016).
- ⁸⁹E. D. H. S. Knecht, J. S. Kielberg, H. J. A. Jensen, and M. Reiher, *J. Chem. Phys.* **142**, 224108 (2015).
- ⁹⁰A. J. Garza, C. A. Jiménez-Hoyos, and G. E. Scuseria, *J. Chem. Phys.* **140**, 244102 (2014).
- ⁹¹S. J. Stoneburner, D. G. Truhlar, and L. Gagliardi, *J. Chem. Phys.* **148**, 064108 (2018).
- ⁹²A. D. Becke, *Phys. Rev. A* **38**, 3098 (1988).
- ⁹³J. P. Perdew, *Phys. Rev. B* **33**, 8822 (1986).
- ⁹⁴J. Tao, J. P. Perdew, V. N. Staroverov, and G. E. Scuseria, *Phys. Rev. Lett.* **91**, 146401 (2003).
- ⁹⁵J. Tao, J. P. Perdew, V. N. Staroverov, and G. E. Scuseria, *Phys. Rev. Lett.* **91**, 146401 (2003).
- ⁹⁶V. N. Staroverov, G. E. Scuseria, J. Tao, and J. P. Perdew, *J. Chem. Phys.* **119**, 12129 (2003).
- ⁹⁷A. D. Becke, *J. Chem. Phys.* **98**, 5648 (1993).
- ⁹⁸C. Lee, W. Yang, and R. G. Parr, *Phys. Rev. B* **37**, 785 (1988).
- ⁹⁹B. Miehlich, A. Savin, H. Stoll, and H. Preuss, *Chem. Phys. Lett.* **157**, 200 (1989).
- ¹⁰⁰A. Schäfer, H. Horn, and R. Ahlrichs, *J. Chem. Phys.* **97**, 2571 (1992).
- ¹⁰¹A. Schäfer, C. Huber, and R. Ahlrichs, *J. Chem. Phys.* **100**, 5829 (1994).

- ¹⁰²F. Weigend and R. Ahlrichs, *Phys. Chem. Chem. Phys.* **7**, 3297 (2005).
- ¹⁰³F. Weigend, *Phys. Chem. Chem. Phys.* **8**, 1057 (2006).
- ¹⁰⁴S. Grimme, J. Antony, S. Ehrlich, and H. Krieg, *J. Chem. Phys.* **132**, 154104 (2010).
- ¹⁰⁵E. Ruiz, J. Cano, S. Alvarez, and P. Alemany, *J. Comput. Chem.* **20**, 1391 (1999).
- ¹⁰⁶I. de P. R. Moreira and F. Illas, *Phys. Chem. Chem. Phys.* **8**, 1645 (2006).
- ¹⁰⁷J. Perdew, A. Savin, and K. Burke, *Phys. Rev. A* **51**, 4531 (1995).
- ¹⁰⁸C. Jacob and M. Reiher, *Int. J. Quantum Chem.* **112**, 3661 (2012).
- ¹⁰⁹A. J. Cohen, D. J. Tozer, and N. C. Handy, *J. Chem. Phys.* **126**, 214104 (2007).
- ¹¹⁰J. Wang, A. D. Becke, and V. H. Smith, Jr., *J. Chem. Phys.* **102**, 3477 (1995).
- ¹¹¹G. E. W. Bauer, *Phys. Rev. B* **27**, 5912 (1983).
- ¹¹²A. Görling, M. Levy, and J. P. Perdew, *Phys. Rev. B* **47**, 1167 (1993).
- ¹¹³E. R. Davidson and A. E. Clark, *Int. J. Quantum Chem.* **103**, 1 (2005).
- ¹¹⁴J.-P. Malrieu and G. Trinquier, *J. Phys. Chem. A* **116**, 8226 (2012).